Zornberg, J. G. (2002). *Géotechnique* **52**, No. 8, 593–604

Discrete framework for limit equilibrium analysis of fibre-reinforced soil

J. G. ZORNBERG*

A methodology is proposed for the design of fibre-reinforced soil slopes using a discrete framework. The analysis of fibre-reinforced soil using traditional composite approaches requires the implementation of laboratory testing programmes on composite fibre-reinforced soil specimens to characterise the material properties. Instead, the analysis of fibre-reinforced soil using a discrete approach can be conducted by independent characterisation of soil specimens and of fibre specimens, since the contributions of soil and fibres are treated separately. A fibre-induced distributed tension can be defined for use in limit equilibrium analysis using the proposed discrete framework. The fibre-induced distributed tension is a function of the volumetric fibre content and tensile strength of individual fibres when failure is induced by fibre breakage. Instead, when failure is induced by fibre pullout, the fibre-induced distributed tension is a function of the volumetric fibre content, interface shear strength and fibre aspect ratio. A critical normal stress, which defines whether the reinforced soil behaviour is governed by pullout or by breakage of the fibres, can be defined analytically using the proposed framework. An experimental testing programme involving tensile testing of fibres as well as triaxial testing of unreinforced and fibre-reinforced specimens was undertaken to validate the proposed framework. As predicted by the discrete framework, the fibre-induced distributed tension was observed to be proportional to the fibre content and fibre aspect ratio when failure was characterised by pullout of individual fibres. The discrete framework predicted accurately the contribution of randomly distributed fibres for the various soil types, fibre aspect ratios and fibre contents considered in the experimental testing programme.

KEYWORDS: design; geosynthetics; reinforced soils; shear strength; soil stabilisation

Nous proposons une méthodologie pour la conception de talus de sol renforcé aux fibres utilisant un cadre de travail discret. L'analyse des sols renforcés aux fibres utilisant des méthodes composites traditionnelles demande la mise en uvre de programmes d'essai en laboratoire sur des spécimens de sol composite renforcé aux fibres pour caractériser les propriétés matérielles. Au lieu de cela, l'analyse du sol renforcé aux fibres utilisant une méthode discrète peut être faite par une caractérisation indépendante de spécimens de sol et de spécimens de fibres, étant donné que les contributions du sol et des fibres sont traitées séparément. Une tension répartie produite par les fibres peut être définie pour être utilisée dans les analyses d'équilibre limite en utilisant le cadre de travail discret que nous proposons. La tension répartie produite par les fibres est une fonction du contenu volumétrique en fibres et de la résistance à la rupture par traction des fibres individuelles lorsque la défaillance est causée par la cassure des fibres. Au lieu de cela, quand la défaillance est causée par l'arrachage des fibres, la tension répartie produite par les fibres est une fonction du contenu volumétrique en fibres, de la résistance au cisaillement de l'interface et du rapport d'allongement des fibres. Une contrainte critique normale, qui détermine si le comportement du sol renforcé, est gouvernée par l'arrachage ou par la cassure des fibres, peut être définie de manière analytique en utilisant le cadre de travail proposé. Nous avons mené un programme d'essais expérimentaux, avec essais de traction des fibres et essais triaxiaux sur des spécimens non renforcés et des spécimens renforcés aux fibres afin de valider le cadre de travail proposé. Comme le cadre de travail proposé l'annonçait, nous avons observé que la tension répartie produite par les fibres était proportionnelle au contenu en fibres et au rapport d'allongement des fibres quand la défaillance était caractérisée par l'arrachage de fibres individuelles. Le cadre de travail discret prédit avec exactitude la contribution des fibres réparties au hasard pour les divers types de sol, rapports d'allongement des fibres et contenus en fibres considérés dans le programme d'essais expérimentaux.

INTRODUCTION

A discrete approach for the design of fibre-reinforced soil slopes is proposed to characterise the contribution of randomly distributed fibres to stability. The design of fibre-reinforced soil slopes has typically been performed using composite approaches, in which the fibre-reinforced soil is considered to be a single homogenised material. Accordingly, fibre-reinforced soil design has required laboratory testing of composite fibre-reinforced soil specimens. Instead, in the discrete approach proposed herein, fibre-reinforced soil is characterised as a two-component (soil and fibres) material. The proposed methodology treats the fibres as discrete elements that contribute to stability by mobilising tensile stresses along the shear plane. Consequently, independent testing of soil specimens and of fibre specimens, but not of fibre-reinforced soil specimens, is used to characterise fibre-reinforced soil performance. Avoiding testing of fibre-reinforced soil specimens is a major objective of the proposed approach since the need to test composite specimens in design has discouraged the implementation of fibre reinforcement in engineering practice.

The composite approach traditionally used in the design of fibre-reinforced soil structures assumes that the contribution of fibres to stability leads to an increase in the shear strength of the 'homogenised' composite reinforced mass. However, as in the case of continuous planar reinforcements (e.g. geogrids, geotextiles), reinforcing fibres actually work in tension and not in shear. Consequently, a discrete approach would also provide a more consistent representation

Manuscript received 24 September 2001; revised manuscript accepted 22 July 2002.
Discussion on this paper closes 1 May 2003, for further details see p. ii.
* Department of Civil, Environmental and Architectural Engineering, University of Colorado at Boulder, USA.

of fibres' contribution to stability than a composite approach would.

After presenting an overview of previous work on fibre-reinforced soil, this paper describes the discrete framework proposed for quantification of the fibre-induced distributed tension. The characteristics of the experimental component of this study are discussed next: this involved tensile testing of fibres and triaxial testing of unreinforced and fibre-reinforced specimens. Finally, the ability of the discrete approach to predict failure of fibre-reinforced soil is evaluated for different soil types, fibre aspect ratios and fibre contents.

BACKGROUND

Past investigations involving fibre-reinforced soil

Traditional soil-reinforcing techniques involve the use of continuous planar inclusions oriented in a preferred direction to enhance stability. In the early stages of development of soil-reinforcement techniques, composite approaches were attempted for the design of planar soil-reinforcement systems. Even though reinforcement inclusions work in tension, composite approaches quantify their contribution to stability as an increased shear strength (e.g. an increased cohesion) within the reinforced soil mass. Subsequently, the contribution of continuous planar inclusions to stability was quantified by discrete approaches in which reinforcement-induced tensile forces were explicitly considered in limit equilibrium analyses. Because discrete approaches characterised reinforced soil behaviour more accurately, geotechnical designers gained better understanding of the contribution of continuous geosynthetic products, which led to cost-effective projects. In addition, the use of discrete approaches facilitated the optimisation of geosynthetic reinforcements because manufacturers could focus on the properties of their products rather than on the properties of composite soil materials. Currently, soil structures reinforced with continuous inclusions are no longer designed using composite approaches.

Unlike soil structures reinforced with planar inclusions, soil structures reinforced with randomly distributed fibres are still conventionally designed using composite approaches. However, the use of composite approaches has possibly prevented both the proper characterisation of the fibres' contribution to stability and the optimisation of fibre products. In addition, the use of composite approaches requires shear strength testing of fibre-reinforced soil specimens to define the properties needed for design.

Relevant contributions have been made on the behaviour of fibres. The advantages of randomly distributed fibres over continuous inclusions include the maintenance of strength isotropy and the absence of the potential planes of weakness that can develop parallel to continuous planar reinforcement elements (Gray & Al-Refeai, 1986; Maher & Gray, 1990; Consoli *et al*., 1998). Micro-reinforcement techniques for soils also include Texol, which consists of monofilament fibres injected randomly into sand (Leflaive, 1985), and randomly distributed polymeric mesh elements (McGown *et al.*, 1985; Morel & Gourc, 1997). The use of fibre-reinforced clay backfill to mitigate the development of tension cracks has also been evaluated (Maher & Ho, 1994). However, as in the case of continuous planar inclusions, the use of fibres to reinforce poorly draining fills deserves careful drainage evaluation (Zornberg & Mitchell, 1994; Mitchell & Zornberg, 1995).

Several composite models have been proposed to explain the behaviour of randomly distributed fibres within a soil mass. The proposed models have been based on mechanistic approaches (Maher & Gray, 1990), on energy dissipation approaches (Michalowski & Zhao, 1996), and on statistics-based approaches (Ranjan *et al.*, 1996). The mechanistic models proposed by Gray & Ohashi (1983) and Maher & Gray (1990) quantify the 'equivalent shear strength' of the fibre-reinforced composite as a function of the thickness of the shear band that develops during failure. The information needed to characterise shear band development for these models is, however, difficult to quantify (Shewbridge & Sitar, 1990). Common findings from the various testing programmes implemented to investigate composite models include the following:

(*a*) Randomly distributed fibres provide strength isotropy in a soil composite.
(*b*) Fibre inclusions increase the 'equivalent' shear strength within a reinforced soil mass.
(*c*) The 'equivalent' strength typically shows a bilinear behaviour, which was experimentally observed by testing of comparatively weak fibres under a wide range of confining stresses.

Slope stabilisation using fibre reinforcement

Slope stabilisation projects can involve either fibre reinforcement or continuous planar reinforcement. Cost, product availability, and standards of practice are significant factors considered when selecting stabilisation methods for a specific project. In some slope stabilisation applications, though, the use of fibre reinforcement provides clear advantages over the use of continuous planar reinforcements. One such application is the stabilisation of thin soil veneers, where a small cohesion value (i.e. shear strength at low confining pressures) has a significant impact on stability. Whereas increased compactive effort can lead to increased shear strength under low confinement, the cohesion increase is often insufficient and deemed unreliable. Instead, fibre reinforcement can provide economically and technically feasible alternatives for veneer stability. A specific example is the potential use of fibre reinforcement for the stabilisation of evapotranspirative cover systems constructed on steep landfill slopes (Zornberg *et al*., 2002). In this application, fibre reinforcement would provide not only increased veneer stability, but also resistance against erosion and desiccation cracking.

Another slope stabilisation application in which fibre reinforcement offers benefits in relation to continuous planar inclusions is in projects involving the localised repair of failed slopes (Gregory & Chill, 1998). In this case, geometric constraints posed by the irregular shape of soil 'patches' make the use of fibre reinforcement an appealing alternative to conventional continuous planar reinforcements. Finally, the use of fibre reinforcement within the soil mass in seismically active areas can significantly increase the yield acceleration used in design. Under dynamic loading conditions, the use of fibres in sands has provided increased resistance to liquefaction and a higher dynamic shear modulus (Maher & Woods, 1990). The use of fibre reinforcement could fulfil an old dream of the geotechnical engineer: a cohesive material with high hydraulic conductivity (Giroud, 1986).

DISCRETE FRAMEWORK FOR FIBRE REINFORCEMENT

Tensile contribution of fibres

A major objective of the proposed discrete framework is to explicitly quantify the fibre-induced distributed tension, t, which is the tensile force per unit area induced in a soil mass by randomly distributed fibres. Specifically, the magnitude of the fibre-induced distributed tension is defined as a

function of the properties of the individual fibres. In this way, as in analyses involving planar reinforcements, limit equilibrium analyses of fibre-reinforced soil can explicitly account for tensile forces.

As in analyses involving planar inclusions, the orientation of the fibre-induced distributed tension should also be identified or assumed. Specifically, the fibre-induced distributed tension can be assumed to act:

(*a*) along the failure surface (Fig. 1), so that the discrete fibre-induced tensile contribution can be directly 'added' to the shear strength contribution of the soil in a limit equilibrium analysis
(*b*) horizontally, which would be consistent with design assumptions for reinforced soil structures using planar reinforcements
(*c*) in a direction somewhere between the initial fibre orientation (which is random) and the orientation of the failure plane.

Even in reinforced soil design using planar reinforcements, the orientation of tensile forces to be used in limit equilibrium analysis is an unsettled issue. However, parametric limit equilibrium analyses (Wright & Duncan, 1991) and centrifuge test results (Zornberg *et al.*, 1998) have shown that the assumed orientation of planar reinforcements does not affect significantly the calculated factor of safety. Since assumption (*a*) simplifies the implementation in limit equilibrium analysis, it is adopted for the framework presented herein.

Definitions

The volumetric fibre content, χ, used in the proposed discrete framework is defined as

$$\chi = \frac{V_f}{V} \tag{1}$$

where V_f is the volume of fibres and V is the control volume of fibre-reinforced soil.

The gravimetric fibre content, χ_w, typically used in construction specifications is defined as

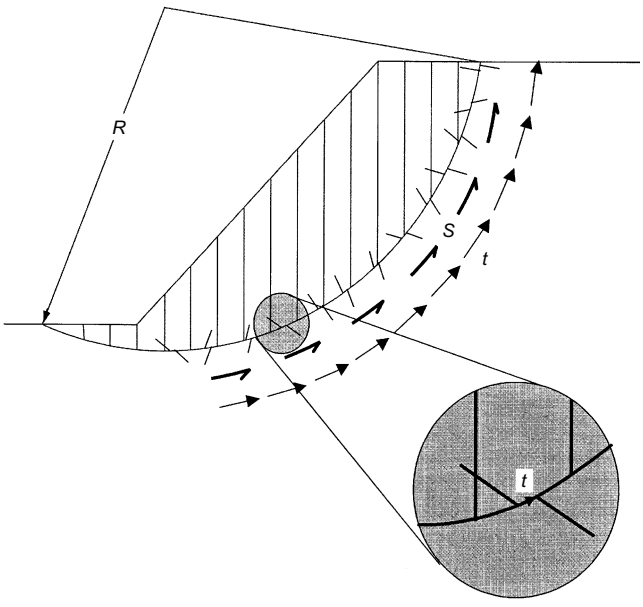

Fig. 1. Schematic failure surface showing fibre-induced distributed tension parallel to failure plane

$$\chi_w = \frac{W_f}{W_s} \tag{2}$$

where W_f is the weight of fibres and W_s is the dry weight of soil. Consistent with engineering practice, the dry weight of soil is used in the definition above instead of the dry weight of fibre-reinforced soil. The definition of gravimetric fibre content is analogous to the classic definition of gravimetric moisture content.

The dry unit weight of the fibre-reinforced soil composite, γ_d, is defined as

$$\gamma_d = \frac{W_f + W_s}{V} \tag{3}$$

From equations (1), (2) and (3) the volumetric fibre content can be defined as

$$\chi = \frac{\chi_w \cdot \gamma_d}{(1 + \chi_w) \cdot G_f \cdot \gamma_w} \tag{4}$$

where G_f is the specific gravity of the fibres and γ_w is the unit weight of water.

Fibre-induced distributed tension when failure is governed by pullout

The distributed tension, t_p, is defined as the fibre-induced distributed tension when failure is governed by pullout (rather than breakage) of individual fibres. The interface shear resistance of individual fibres, f_f, can be characterised as

$$f_f = a + \tan\delta \cdot \sigma_{n,ave} \tag{5}$$

where a is the adhesive component of the interface shear strength between the soil and the polymeric fibre, $\tan\delta$ is the frictional component, and $\sigma_{n,ave}$ is the average normal stress acting on the fibres. The concept of interaction coefficients, commonly used in the soil reinforcement literature for continuous planar reinforcement, is adopted herein to relate the interface shear strength to the shear strength of the soil. The interaction coefficients are defined as

$$c_{i,c} = \frac{a}{c} \tag{6}$$

$$c_{i,\phi} = \frac{\tan\delta}{\tan\phi} \tag{7}$$

where c and $\tan\phi$ are the cohesive and frictional components of the soil shear strength, and $c_{i,c}$ and $c_{i,\phi}$ are the interaction coefficients for the cohesive and frictional components of the interface shear strength. Using equations (5), (6) and (7) the interface shear strength of individual fibres can be expressed as

$$f_f = c_{i,c} \cdot c + c_{i,\phi} \cdot \tan\phi \cdot \sigma_{n,ave} \tag{8}$$

Geosynthetic fibres are typically characterised by their linear density, *ld*, which is generally expressed in deniers (1 denier = 1/9000 g/m). The cross-sectional area of an individual fibre, $A_{f,i}$, can be obtained from the linear density as follows:

$$A_{f,i} = \frac{ld}{G_f \cdot \gamma_w} \tag{9}$$

The equivalent diameter, d_f, of a single fibre is defined for the purposes of this study as

$$d_f = \left(\frac{4A_{f,i}}{\pi}\right)^{1/2} \tag{10}$$

The embedment length of a fibre, l_e, is the length of the shorter portion of the fibre on either side of the failure

surface. The pullout resistance of a fibre of length, l_f should be estimated over the shortest side of the two portions of a fibre intercepted by the failure plane. The length of the shortest portion of a fibre intercepted by the failure plane varies from zero to $l_f/2$. Statistically, the average embedment length of randomly distributed fibres, $l_{e,ave}$, can be analytically defined by

$$l_{e,ave} = \frac{l_f}{4} \tag{11}$$

The average pullout resistance can be quantified along the average embedment length, $l_{e,ave}$, of all individual fibres crossing a soil control surface A. Accordingly, if failure is governed by fibre pullout, the ultimate tensile force, UTF_p, carried by the individual fibres intersecting the control section can be defined using equation (8) as:

$$UTF_p = \alpha \cdot (\pi \cdot d_f \cdot l_{e,ave}) \cdot (c_{i,c} \cdot c + c_{i,\phi} \cdot \tan\phi \cdot \sigma_{n,ave}) \cdot n \tag{12}$$

where n is the number of individual fibres intersecting the control surface A, $(\pi.d_f.l_{e,ave})$ is the average area of a fibre subjected to pullout, and α is an empirical coefficient introduced to account for the effect of fibre orientation. For the case of randomly oriented fibres considered in this study, the coefficient α equals 1, but is included in the formulation to account for the potential effect of preferred orientation of fibres. The number of individual fibres intersecting the control surface can be estimated as

$$n = \frac{A_f}{A_{f,i}} \tag{13}$$

where A_f is the total cross-sectional area of the fibres intersecting the control surface A. The number of individual fibres can also be defined using equation (10) as

$$n = \frac{A_f}{\frac{1}{4}\pi(d_f)^2} \tag{14}$$

The ratio between the total cross-sectional area of the fibres, A_f, and the control surface A is assumed to be defined by the volumetric fibre content, χ. That is:

$$\chi = \frac{A_f}{A} \tag{15}$$

Equation (15) is rigorously valid for the case in which the fibres are oriented perpendicularly to the failure plane. However, test results reported by Gray & Ohashi (1983) provide experimental justification for use of this equation for randomly distributed fibres. In that study, similar shear strength envelopes were reported from direct shear tests performed using fibre-reinforced specimens in which the fibres were either perpendicularly or randomly placed in relation to the shear plane. Finally, the aspect ratio, η, of individual fibres is defined as

$$\eta = \frac{l_f}{d_f} \tag{16}$$

Using the definition of the fibre-induced distributed tension, the ultimate tensile force carried by the fibres intercepting a control surface A when failure is governed by pullout can be estimated as

$$UTF_p = t_p \cdot A \tag{17}$$

By setting equation (12) equal to equation (17) and then incorporating equations (11), (14), (15) and (16), the fibre-induced distributed tension when failure is governed by pullout of the individual fibres can be estimated as

$$t_p = \alpha \cdot \chi \cdot \eta \cdot (c_{i,c} \cdot c + c_{i,\phi} \cdot \tan\phi \cdot \sigma_{n,ave}) \tag{18}$$

Fibre-induced distributed tension when failure is governed by tensile breakage

The distributed tension, t_t, is defined as the fibre-induced distributed tension when failure is governed by fibre breakage (i.e. when the ultimate tensile strength of individual fibres is achieved). The ultimate tensile strength of the individual fibres, $\sigma_{f,ult}$, can be obtained by laboratory tensile testing of individual fibre specimens. The soil itself is assumed to have no tensile strength. Accordingly, when failure is governed by fibre breakage, the ultimate tensile force, UTF_t, carried by all individual fibres intercepting a control section A is

$$UTF_t = \alpha \cdot \sigma_{f,ult} \cdot \sum A_{f,i} = \alpha \cdot \sigma_{f,ult} \cdot A_f \tag{19}$$

Also in this case, an empirical coefficient, α, is included to account for the effect of fibre orientation. This coefficient equals 1 for randomly oriented fibres, which is the focus of this study.

Using the definition of the fibre-induced distributed tension, the ultimate tensile force carried by the fibres intercepting a control surface A when failure is governed by breakage of fibres can be estimated as

$$UTF_t = t_t \cdot A \tag{20}$$

By setting equations (19) and (20) equal to each other, and using equation (15), the fibre-induced distributed tension when failure is governed by tensile breakage of individual fibres can be estimated as

$$t_t = \alpha \cdot \chi \cdot \sigma_{f,ult} \tag{21}$$

Fibre-induced distributed tension

The fibre-induced distributed tension, t, to be used in the discrete approach to account for the tensile contribution of the fibres in limit equilibrium analysis is

$$t = \min(t_p, t_t) \tag{22}$$

Using equations (18), (21) and (22), the fibre-induced distributed tension, t, can also be defined as

$$t = \min[\alpha \cdot \chi \cdot \eta \cdot (c_{i,c} \cdot c + c_{i,\phi} \cdot \tan\phi \cdot \sigma_{n,ave}), \alpha \cdot \chi \cdot \sigma_{f,ult}] \tag{23}$$

Figure 2 shows the bilinear representation of the fibre-induced distributed tension. Note that the fibre-induced distributed tension can be estimated without performing laboratory tests on fibre-reinforced specimens. That is, for a given

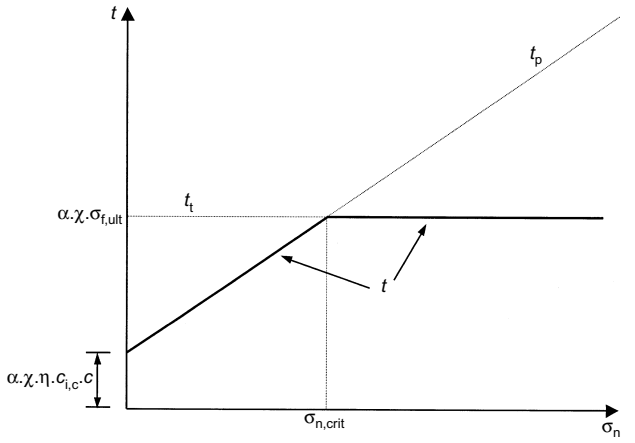

Fig. 2. Representation of fibre-induced distributed tension according to the discrete approach

normal stress, the fibre-induced distributed tension can be estimated, using equation (23), as a function of the fibre content, the fibre geometry, the fibre tensile strength, and the shear strength of the soil. Conservative assumptions on the interaction coefficients can be made for design purposes.

The critical normal stress, $\sigma_{n,crit}$, which defines the change in the governing failure mode, is the normal stress at which failure occurs simultaneously by pullout and tensile breakage of the fibres. That is, the following condition holds at the critical normal stress:

$$t_t = t_p \tag{24}$$

An analytical expression for the critical normal stress can be obtained using equations (18), (21) and (24) as follows:

$$\sigma_{n,crit} = \frac{\sigma_{f,ult} - \eta \cdot c_{i,c} \cdot c}{\eta \cdot c_{i,\phi} \cdot \tan\phi} \tag{25}$$

Equation (25) shows that the critical normal stress is a function of the fibre geometry, the fibre tensile strength, the shear strength of the soil, and the interaction coefficients. However, note that the critical normal stress is not a function of the fibre content. Although past investigations (e.g. Maher & Gray, 1990) have experimentally identified a transition on the shear strength envelope of fibre-reinforced specimens, an analytic formulation for determination of the critical normal stress had not been defined.

Equivalent shear strength of reinforced fibre composites

Triaxial compression tests can be performed to experimentally define the 'equivalent shear strength' of fibre-reinforced composites (e.g. Maher & Gray, 1990; Gregory & Chill, 1998). This section defines the 'equivalent shear strength' of fibre-reinforced specimens as a function of the fibre-induced distributed tension, t. These relationships will be used for validation of the proposed discrete framework against experimental results. As previously mentioned, the proposed discrete framework assumes that fibre-induced distributed tension, t, in a triaxial specimen is parallel to the shear plane (Fig. 3). In this case, the magnitude of the normal stress acting on the shear plane is not affected by the fibre-induced distributed tension, t. Accordingly, the equivalent shear strength of the fibre-reinforced soil, S_{eq}, can be defined as

$$S_{eq} = S + t \tag{26}$$

where S is the shear strength of unreinforced soil. Note that, if the fibre-induced distributed tension t were not parallel to the failure surface, the direct contribution of the fibre reinforcement to the 'equivalent shear strength' would be smaller than in the parallel case. However, the component of the fibre-induced distributed tension perpendicular to the shear plane would induce a local increase in normal stress, which would lead to increased soil shear strength.

If the average normal stress acting on the fibres, $\sigma_{n,ave}$, is below the critical value ($\sigma_{n,ave} < \sigma_{n,crit}$), equation (26) results in:

$$S_{eq,p} = S + t_p \tag{27}$$

where $S_{eq,p}$ is the equivalent shear strength of the fibre-reinforced soil when failure is governed by fibre pullout. Assuming a linear soil shear strength envelope, and using equations (18) and (27):

$$S_{eq,p} = (c + \tan\phi \cdot \sigma_n) + (\alpha \cdot \eta \cdot \chi \cdot c_{i,c} \cdot c + \alpha \cdot \eta \cdot \chi \cdot c_{i,\phi} \cdot \tan\phi \cdot \sigma_{n,ave}) \tag{28}$$

where σ_n is the normal stress acting on the failure plane.

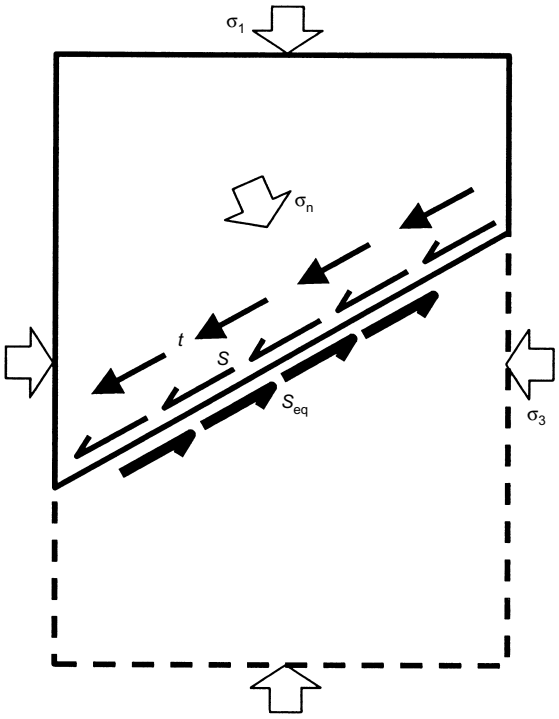

Fig. 3. Schematic representation of the equivalent shear strength in a triaxial fibre-reinforced specimen

Note that the average normal stress acting on the fibres, $\sigma_{n,ave}$, does not necessarily equal σ_n. Since the fibres are randomly oriented, a possible assumption is to estimate $\sigma_{n,ave}$ as the octahedral stress component. In this case, and considering an axisymmetric configuration and a linear soil shear strength envelope:

$$\sigma_{n,ave} = \frac{\sigma_1 + 2\sigma_3}{3} = \left(\frac{1}{\cos\phi \cdot \sin\phi} - \frac{1}{\tan\phi} - \frac{1}{3\cos\phi}\right)c + \left(\frac{1}{\cos^2\phi} - \frac{\sin\phi}{3\cos^2\phi}\right)\sigma_n \tag{29}$$

where σ_1 and σ_3 are the major and minor principal stresses. Alternatively, $\sigma_{n,ave}$ could be assumed to equal the normal stress acting on the failure plane. That is:

$$\sigma_{n,ave} = \sigma_n \tag{30}$$

A sensitivity evaluation was undertaken using typical ranges of shear strength parameters. This evaluation indicated that the equivalent shear strength predicted using equation (28) is not very sensitive to the selection of $\sigma_{n,ave}$ defined by equation (29) or (30). Consequently, and in order to simplify the formulation proposed herein, the assumption stated by equation (30) was adopted. Accordingly, the following expressions result from equations (28) and (30) to define the equivalent shear strength when failure is governed by fibre pullout:

$$S_{eq,p} = c_{eq,p} + (\tan\phi)_{eq,p} \cdot \sigma_n \tag{31}$$

$$c_{eq,p} = (1 + \alpha \cdot \eta \cdot \chi \cdot c_{i,c}) \cdot c \tag{32}$$

$$(\tan\phi)_{eq,p} = (1 + \alpha \cdot \eta \cdot \chi \cdot c_{i,\phi}) \cdot \tan\phi \tag{33}$$

where $c_{eq,p}$ and $(\tan\phi)_{eq,p}$ are equivalent shear strength parameters for the fibre-reinforced soil when the normal stress is below $\sigma_{n,crit}$.

If the average normal stress is above the critical value ($\sigma_{n,ave} > \sigma_{n,crit}$), equation (26) results in

$$S_{eq,t} = S + t_t \tag{34}$$

where $S_{eq,t}$ is the equivalent shear strength of the fibre-reinforced soil when failure is governed by tensile breakage of the fibres. Assuming a linear soil shear strength envelope, and using equations (21) and (34):

$$S_{eq,t} = (\alpha \cdot \chi \cdot \sigma_{f,ult}) + (c + \tan\phi \cdot \sigma_n) \tag{35}$$

Equivalently, the following expressions can be obtained from equation (35) to define the equivalent shear strength when failure is governed by tensile breakage of the fibres:

$$S_{eq,t} = c_{eq,t} + (\tan\phi)_{eq,t} \cdot \sigma_n \tag{36}$$

$$c_{eq,t} = c + \alpha \cdot \chi \cdot \sigma_{f,ult} \tag{37}$$

$$(\tan\phi)_{eq,t} = \tan\phi \tag{38}$$

where $c_{eq,t}$ and $(\tan\phi)_{eq,t}$ are equivalent shear strength parameters for the fibre-reinforced soil when the normal stress is above $\sigma_{n,crit}$.

Figure 4 illustrates the bilinear representation for the equivalent shear strength envelope obtained using the discrete framework. Equations (31) and (36) define the linear expressions of the two portions of the bilinear envelope below and above $\sigma_{n,crit}$ respectively. As previously mentioned, the magnitude of the equivalent shear strength is defined as a function of the (unreinforced) soil shear strength properties and the fibre properties. That is, the parameters defining the equivalent shear strength of the fibre-reinforced soil composite could be defined without undertaking testing of soil fibre composite specimens.

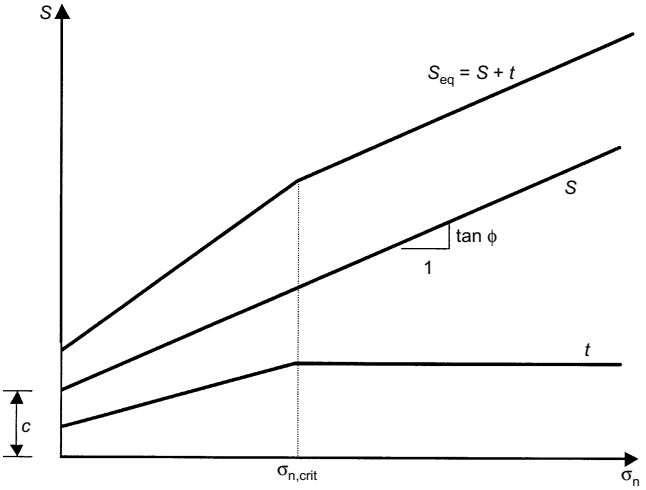

Fig. 4. Representation of the equivalent shear strength according to the discrete approach

EXPERIMENTAL VALIDATION

Tensile testing programme of individual fibres

A tensile testing programme on polypropylene fibres was implemented as part of this investigation. The scope of the tensile testing programme included a sensitivity evaluation of the effect of loading rate and gauge length on the tensile strength of individual fibres. A series of baseline tests were performed in general accordance with ASTM D2256–97 (ASTM, 1997). The standard test is performed using a loading rate of 300 mm/min and a gauge length of 250 mm. In order to evaluate the sensitivity of the tensile strength results, additional tests were performed using a loading rate of 25 mm/min and a gauge length of 75 mm. The tests were performed using polypropylene fibres with linear densities of 2610 and 360 deniers, which correspond to linear density values of the fibres used in the triaxial testing programme. A total of eight tensile test series were performed (two fibre linear densities, two loading rates, two gauge lengths).

Table 1 presents a summary of the tensile strength results. The results reported in the table for each series are the average of results obtained from three tensile tests. The results indicate that, for the two polypropylene fibres used in this study, tensile strength is not very sensitive to the loading rate, gauge length or, to some degree, the linear density. The average tensile strength is approximately 425 000 kPa. Tensile strength values of this order of magnitude lead to critical normal stress values (equation (25)) that are significantly higher than the stresses anticipated in typical geotechnical projects. Accordingly, because of the comparatively high tensile strength of the individual fibres, significant confinement is needed to induce tensile breakage of the individual fibres.

Triaxial testing programme: general approach

Triaxial tests were conducted in this investigation to validate the proposed discrete framework for fibre-reinforced soils. The tests were conducted using commercially available polypropylene fibres and different soil types, fibre contents and fibre aspect ratios. The tests were conducted as part of the characterisation programmes of actual projects that considered the use of polypropylene fibres for slope stabilisation.

The proposed discrete framework is consistent with the behaviour reported for fibre-reinforced soil specimens tested under stresses above the critical value. Previous investigators (e.g. Maher & Gray, 1990) have reported the following observations regarding the magnitude of the critical normal stress:

(*a*) An increase in fibre aspect ratio results in a lower critical stress.
(*b*) An increase in fibre content shows no apparent change in the critical stress.

Table 1. Summary of fibre tensile strength test results

Series no.†	Fibre linear density: deniers‡	Loading rate: mm/min	Gauge length: mm	Tensile strength: kPa	Strain at peak stress: %
1	2610	300	250	372 703	9·97
2	2610	25	250	374 883	11·62
3	2610	300	75	439 356	16·23
4	2610	25	75	378 117	16·35
5	360	300	250	470 854	15·27
6	360	25	250	434 645	17·87
7	360	300	75	477 533	19·24
8	360	25	75	454 331	22·47

† The reported test results for each series correspond to the average of three tensile tests.
‡ 1 denier = 1/9000 g/m.

(*c*) Soils with comparatively high shear strength result in a lower critical stress.

These experimental observations can be explained by equation (25), obtained using the discrete framework proposed herein. Also, reported experimental results for tests conducted above the critical normal stress have indicated that the fibre-reinforced shear strength envelope is parallel to the unreinforced shear strength envelope (Maher & Gray, 1990; Ranjan *et al.*, 1996). These experimental observations can be explained by equations (36)–(38), which were also obtained using the discrete framework proposed herein. However, fibre pullout is the governing failure mode for the polymeric fibres used in this investigation because of the comparatively high tensile strength and comparatively short length of the fibres. Accordingly, the triaxial testing programme conducted in this study focuses only on the first portion of the bilinear strength envelope shown in Fig. 4, which corresponds to the stress range of practical interest when using the polymeric fibres available on the market.

Triaxial tests using Soil 1, which classifies as CL according to USCS, were conducted to evaluate the potential stabilisation of a landfill cover system. Table 2 shows the characteristics of Soil 1. Fibrillated polypropylene fibres with a linear density of 2610 deniers and fibre lengths of 25 mm and 50 mm were used in the experimental testing programme. The gravimetric fibre contents used in the testing programme were 0·2% and 0·4%. In addition, triaxial tests were conducted using control (unreinforced) soil specimens. The maximum dry unit weight for the unreinforced soil was 15·5 kN/m^3 and the optimum moisture content was 22·5% according to the ASTM D698 test (Standard Proctor compaction test; ASTM, 2000). Remoulded specimens for triaxial testing were prepared at a target dry unit weight of 13·9 kN/m^3 (90% of maximum) and at the optimum moisture content.

The triaxial testing programme involved backpressure saturated ICU triaxial tests with measurement of pore water pressure. The tests were performed in general accordance with ASTM D4767 using 71 mm diameter specimens with a minimum length-to-diameter ratio of 2. A total of five series of triaxial tests were conducted. Table 3 presents a summary of the characteristics of these series (Series 1 to 5). Consistent with confinement representative of cover systems, the shear strength envelope was defined using specimens tested at confining pressures of 24, 48 and 96 kPa. The unreinforced tests (Series 1) yielded an effective shear strength envelope defined by a cohesion of 12·2 kPa and a friction angle of 31·2° (Table 3).

Selection of the interaction coefficients used in the analysis was based on results obtained from a pullout testing programme conducted using woven geotextiles manufactured by the provider of the fibres used in this study. The testing programme involved four woven geotextiles tested using four normal stresses (16 individual pullout tests). The tests were conducted in general accordance with Standard Test Method D6706-01; ASTM, 2001 using a CL soil. The average interaction coefficient obtained from these tests was 0·81, and

Table 2. Summary of soil properties

Property	Soil 1	Soil 2	Soil 3	Soil 4	Soil 5	Soil 6
USCS Classification	CL	SP	CL	CL	SM	CH
LL: %	49·0	–	48·0	46·0	–	80·0
PL: %	24·0	–	21·0	19·0	–	26·0
IP: %	25·0	–	27·0	27·0	–	54·0
% fines	82·6	1·4	96·8	77·0	19·0	98·4

Table 3. Summary of predictions using the discrete framework

Series no.	Soil type	Fibre linear density: deniers	Fibre length: mm	Fibre content, χ_w: %	Equivalent cohesion: kPa†, ‡, §	Equivalent friction angle: degrees‡, §, ¶
1	Soil 1	–	–	0·0	12·2	31·2
2	Soil 1	2610	50	0·2	14·3	35·7
3	Soil 1	2610	50	0·4	16·6	39·9
4	Soil 1	2610	25	0·2	13·1	33·4
5	Soil 1	2610	25	0·4	14·3	35·7
6	Soil 2	–	–	0·0	6·1	34·3
7	Soil 2	360	50	0·2	9·8	47·5
8	Soil 2	360	50	0·4	13·5	56·3
9	Soil 2	360	25	0·2	8·0	41·6
10	Soil 2	360	25	0·4	9·8	47·5
11	Soil 3	–	–	0·0	11·2	26·2
12	Soil 3	2610	50	0·2	13·9	31·2
13	Soil 4	–	–	0·0	10·5	24·1
14	Soil 4	2610	50	0·2	12·9	28·7
15	Soil 5	–	–	0·0	5·6	35·8
16	Soil 5	2610	50	0·2	6·6	41·7
17	Soil 6	–	–	0·0	28·8	11·2
18	Soil 6	2610	50	0·2	34·6	13·4

† Equivalent cohesion of fibre-reinforced specimens was calculated using equation (32). Cohesion reported for unreinforced series ($\chi_w = 0{\cdot}0\%$) was defined from experimental data.
‡ Interaction coefficients assumed for all predictions as: $c_{i,c} = 0{\cdot}8$ and $c_{i,\phi} = 0{\cdot}8$.
§ Coefficient α was assumed equal to 1·0 for all predictions.
¶ Equivalent friction angle of fibre-reinforced specimens was calculated using equation (33). Friction angle reported for unreinforced series ($\chi_w = 0{\cdot}0\%$) was defined from experimental data.

the scatter of the individual results was considerably low (standard deviation for the interaction coefficient was 0·055). The interface shear strength obtained from pullout test results conducted on woven geotextiles was considered representative of the interface shear strength on individual fibres. Accordingly, interaction coefficients of 0·8 are assumed in the analyses conducted in this study. For practical purposes, interaction coefficients can be selected from values reported in the literature for continuous planar reinforcements. This is because pullout tests conducted using a variety of soils and planar geosynthetics have been reported to render interaction coefficient values falling within a narrow range (Koutsourais *et al.*, 1998).

The following steps illustrate the general approach followed to predict the equivalent shear strength of triaxial test Series 2:

(*a*) *Determination of the volumetric fibre content,* χ. A volumetric fibre content of 0·0031 (0·31%) is obtained from equation (4) using $G_f = 0{\cdot}91$, $\chi_w = 0{\cdot}002$, and $\gamma_d = 13{\cdot}9$ kN/m^3.

(*b*) *Determination of the fibre aspect ratio,* η. A fibre aspect ratio of 79·73 is calculated from equations (9), (10) and (16) using $ld = 2610$ deniers, $G_f = 0{\cdot}91$, and $l_f = 50$ mm. Although the equivalent diameter defined by equation (10) is used in this study, the effect of fibrillation used in fibre manufacturing may deserve further evaluation.

(*c*) *Determination of the critical normal stress,* $\sigma_{n,crit}$. A critical normal stress of approximately 11 000 kPa is calculated from equation (25) using $\sigma_{f,ult} = 425\,000$ kPa, $\eta = 79{\cdot}73$, shear strength properties of Soil 1 (Table 3), and assuming $c_{i,c} = c_{i,\phi} = 0{\cdot}8$. For a soil unit weight of 13·9 kN/m^3, the calculated critical normal stress corresponds to a 790 m high soil column. As anticipated, the critical normal stress is beyond the range of most practical applications.

(*d*) *Determination of the equivalent shear strength,* S_{eq}. The equivalent shear strength for the range of normal stresses of interest is obtained using equations (31), (32) and (33). As the fibres were mixed in the laboratory, they are considered randomly distributed (i.e. $\alpha = 1{\cdot}0$). The values of the other parameters are those described previously. As indicated in Table 3 (Series 2), the predicted cohesive component of the equivalent shear strength is 14·3 kPa and the predicted equivalent friction angle is 35·7°.

Figure 5 shows the shear strength results obtained from unreinforced specimens (Series 1) and those obtained using specimens reinforced with 50 mm long fibres placed at a gravimetric fibre content of 0·2% (Series 2). Best fit of fibre-reinforced experimental data points leads to an effective shear strength envelope characterised by a cohesion of 15·7 kPa and a friction angle of 34·6°. The experimental results show that the use of fibres leads to a clear increase in the equivalent shear strength. The figure also shows the equivalent shear strength envelope predicted using the proposed discrete framework following the steps described above. Coefficients of interaction equal to 0·8 are consistent with the pullout testing programme. However, a parametric evaluation is shown in the figure, which shows the predicted equivalent shear strength envelopes obtained using interaction coefficients ranging from 0·6 to 1·0. Very good agreement can be observed between the fibre-reinforced experimental data points and the predicted shear strength envelopes, particularly when considering interaction coefficients consistent with pullout test results.

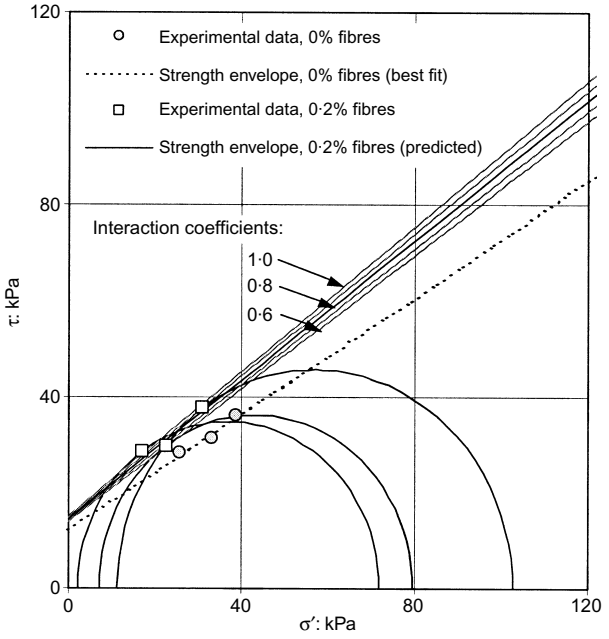

Fig. 5. Comparison between predicted and experimental shear strength results for specimens of Soil 1 with 50 mm fibres placed at $\chi_w = 0{\cdot}2\%$. Shear strength envelope for unreinforced specimens also shown. Mohr circles shown for reinforced specimens only. Predicted envelopes are shown for interaction coefficients ranging from 0·6 to 1·0

Triaxial testing programme: effect of fibre content and fibre aspect ratio

The same approach as used to predict the equivalent shear strength for Series 2 was followed to predict the equivalent shear strength for the other test series conducted in this study. Specifically, Series 3 was conducted using Soil 1 and the same 50 mm long fibres as in Series 2, but with a gravimetric fibre content of 0·4%. The predicted parameters that define the equivalent shear strength in this case are indicated in Table 3 (Series 3). Fig. 6 shows the experimental data obtained from triaxial tests conducted on Soil 1

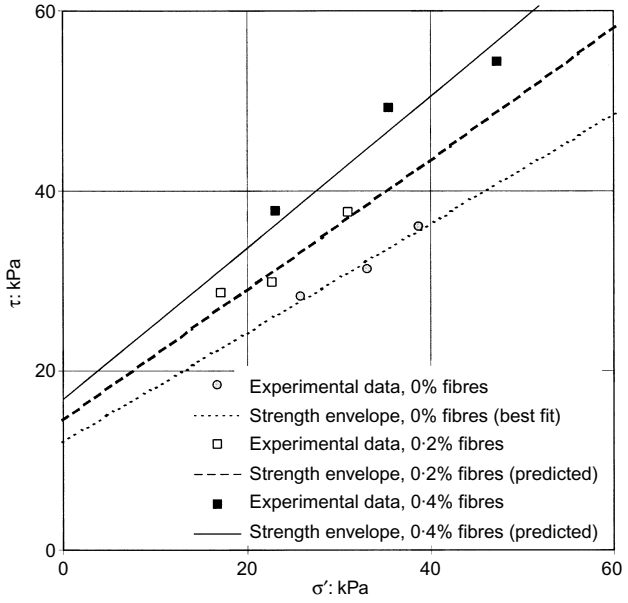

Fig. 6. Comparison between predicted and experimental shear strength results for specimens of Soil 1 with 50 mm fibres placed at $\chi_w = 0{\cdot}0\%$, 0·2%, 0·4%

using 50 mm long fibres placed at gravimetric fibre contents of 0·0%, 0·2% and 0·4%. The experimental results show a clear increase in equivalent shear strength with increasing fibre content. The shear strength envelope shown in the figure for unreinforced soil was defined by fitting the experimental data. However, the shear strength envelopes shown for fibre-reinforced soil were predicted analytically using the proposed discrete framework. Very good agreement can be observed between the experimental data points and the predicted shear strength envelopes. As predicted by the discrete framework, the distributed fibre-induced tension increases linearly with the volumetric fibre content.

The effect of fibre aspect ratio is illustrated in Fig. 7, which compares the experimental and predicted shear strength envelopes obtained for Soil 1 but using shorter (25 mm long) fibres than in Series 2 and 3. The results shown in the figure correspond to fibre contents of 0·0% (Series 1), 0·2% (Series 4), and 0·4% (Series 5). The parameters predicted in this case for the equivalent shear strength of fibre-reinforced soil are also indicated in Table 3. Because of the smaller aspect ratio of the fibres in these series, the fibre-induced contribution is smaller than that obtained in Series 2 and 3 for the same soil and fibre contents. In this case, very good agreement can also be observed between the experimental data points and the predicted shear strength envelopes. As predicted by the discrete framework, the distributed fibre-induced tension increases linearly with the fibre aspect ratio.

A comprehensive testing programme using a sandy soil (USCS classification SP) was conducted to further validate the effect of fibre content and fibre aspect ratio using the proposed discrete approach. The characteristics of this soil are summarised in Table 2 (Soil 2). The linear density of the fibres used in this testing programme is 360 deniers. Both fibrillated and regular (tape) fibres were used in the study. The fibrillation manufacturing process induces longitudinal cuts in the fibres. As in the previously described test series, the triaxial testing programme involved backpressure-saturated ICU triaxial tests with measurement of pore water pressure. A total of five triaxial test series were conducted using Soil 2 (Series 6–10 in Table 3). Each series typically included six specimens (three using fibrillated fibres and three using tape fibres). The shear strength envelope for each series was defined using the results of specimens tested at confining pressures of 35·15, 70·31 and 140·62 kPa. The control (unreinforced) series yielded an effective shear strength defined by a cohesion of 6·1 kPa and a friction angle of 34·3° (Series 6).

The effect of fibre content using Soil 2 is shown in Fig. 8, which compares the experimental data and predicted shear strength envelopes obtained using 50 mm long fibres placed at fibre contents of 0·0% (Series 6), 0·2% (Series 7), and 0·4% (Series 8). Consistent with the Soil 1 results, the experimental results obtained using Soil 2 show a clear increase in equivalent shear strength with increasing fibre content. No major influence of fibrillation is perceived in the results of the testing programme. The shear strength envelope for the unreinforced specimens was defined by fitting the experimental data. However, the shear strength envelopes shown in the figure for the reinforced specimens were predicted analytically using the proposed discrete framework. The predicted shear strength parameters are indicated in Table 3. Very good agreement is observed between the experimental data points and the predicted shear strength envelopes.

The effect of fibre aspect ratio using Soil 2 is shown in Fig. 9, which compares the experimental and predicted shear strength envelopes obtained for Soil 2, but using shorter (25 mm long) fibres. Consistent with the previously described set of tests, the fibres were placed at fibre contents of 0·0% (Series 6), 0·2% (Series 9), and 0·4% (Series 10). The fibre-induced contribution is smaller than that obtained in Series 7 and 8 for the same soil and fibre because of the smaller fibre aspect ratio. No major influence of fibrillation is perceived in the results of the testing programme. The parameters predicted in this case for the equivalent shear strength of fibre-reinforced soil are also indicated in Table 3. Also in the test series shown in this figure, very good agreement can be observed between the experimental data points and the predicted shear strength envelopes.

Additional insight into the validity of the proposed discrete approach can be obtained by comparing the results obtained for specimens reinforced with 50 mm long fibres placed at a fibre content of 0·2% with those obtained for specimens reinforced with 25 mm long fibres placed at a

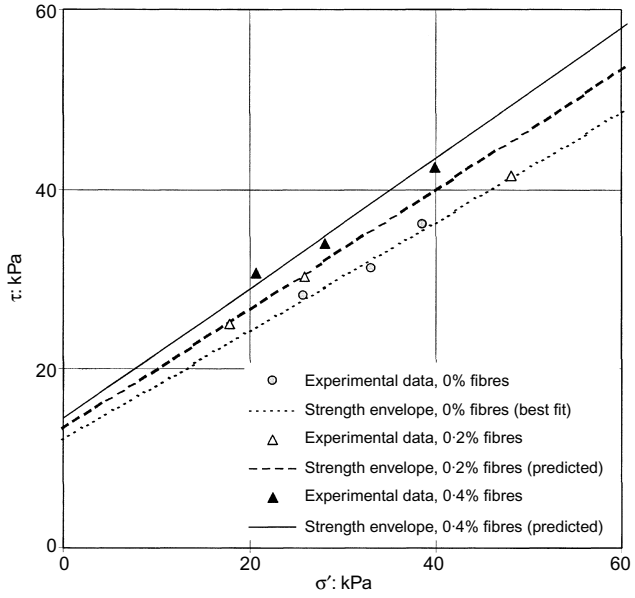

Fig. 7. Comparison between predicted and experimental shear strength results for specimens of Soil 1 with 25 mm fibres placed at $\chi_w = 0{\cdot}0\%, 0{\cdot}2\%, 0{\cdot}4\%$

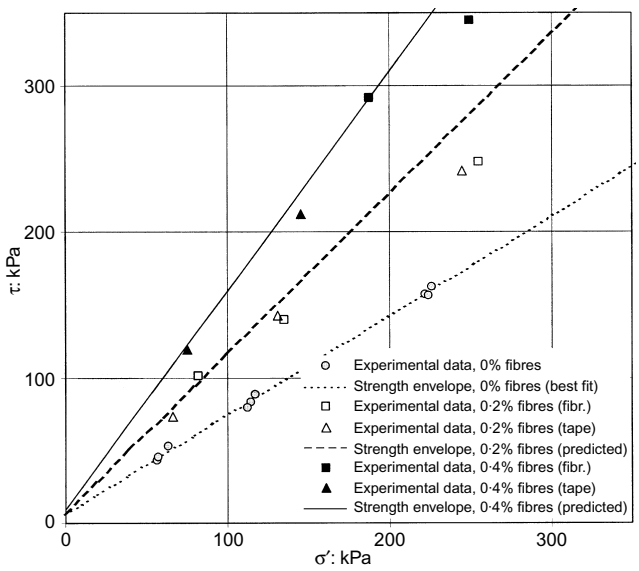

Fig. 8. Comparison between predicted and experimental shear strength results for specimens of Soil 2 with 50 mm fibres placed at $\chi_w = 0{\cdot}0\%, 0{\cdot}2\%, 0{\cdot}4\%$

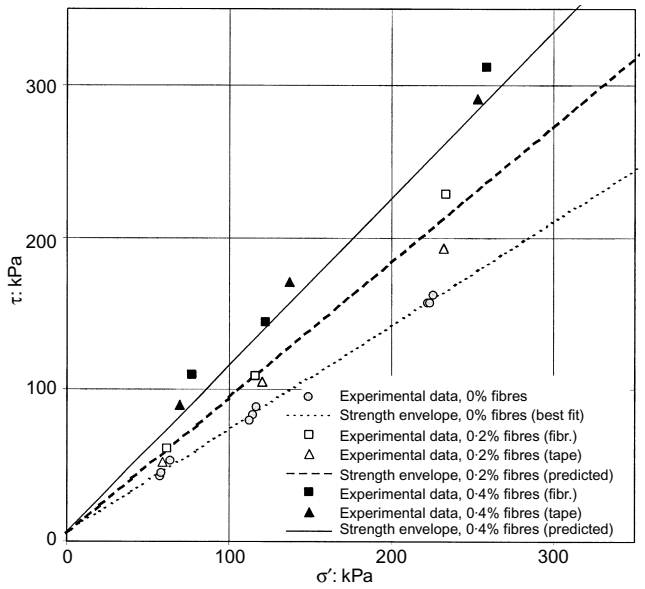

Fig. 9. Comparison between predicted and experimental shear strength results for specimens of Soil 2 with 25 mm fibres placed at $\chi_w = 0{\cdot}0\%$, 0·2%, 0·4%

fibre content of 0·4%. As inferred from inspection of equation (18), the fibre-induced distributed tension is directly proportional to both the fibre content and the fibre aspect ratio. Consequently, the predicted equivalent shear strength parameters for the above combinations of fibre length and fibre content are the same (see equivalent parameters in Table 3 for Series 2, 5, 7 and 10). Fig. 10 consolidates these experimental results. The good agreement between experimental results and predicted values provides additional evidence of the suitability of the proposed discrete approach. From the practical standpoint, note that the use of 50 mm long fibres placed at a fibre content of 0·2% corresponds to half the reinforcement material compared with the use of 25 mm long fibres placed at a fibre content of 0·4%. That is, for the same target equivalent shear strength the first combination leads to half the material costs of the second one. It is anticipated, though, that difficulty in achieving good fibre mixing may compromise the validity of the relationships developed herein for comparatively high aspect ratios (i.e. comparatively long fibres) and for comparatively high fibre contents. The fibre content or fibre length at which the validity of these relationships is compromised should be further evaluated. Nonetheless, good mixing was achieved for the fibre contents and fibre lengths considered in this investigation, which were selected based on values typically used in geotechnical projects.

Triaxial testing programme: suitability of different soil types

Additional series of triaxial tests were conducted using soil types not contemplated in the previous test series in order to assess the validity of the proposed discrete approach for other soils typical of embankment and cover system projects. Four additional materials were evaluated in this study, including materials that classify as CL, SM and CH. The characteristics of these soils are shown in Table 2 (Soils 3, 4, 5 and 6). The experimental unreinforced shear strength envelope was obtained for each soil type. Also, tests were conducted on fibre-reinforced specimens prepared using 50 mm long fibres placed at a gravimetric fibre content of 0·2%. The linear density of the fibres used in these test series is 2610 deniers. The test results obtained as part of this experimental component are shown in Fig. 11. The

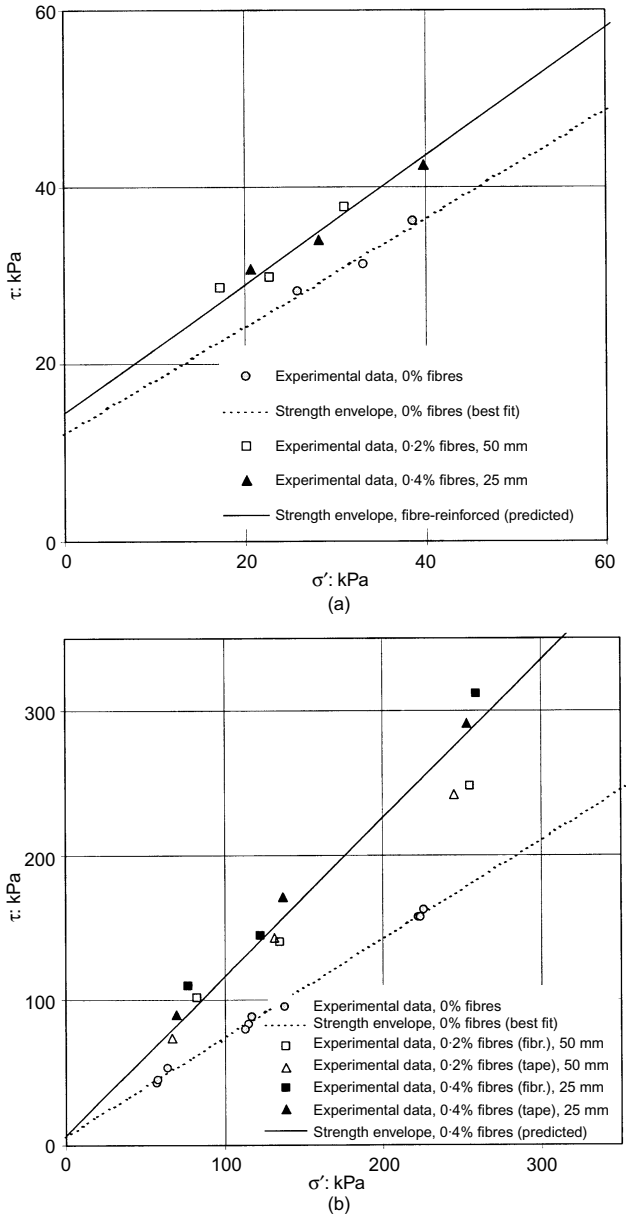

Fig. 10. Consolidated shear strength results for specimens reinforced with 50 mm fibres placed at $\chi_w = 0{\cdot}2\%$ and 25 mm fibres placed at $\chi_w = 0{\cdot}4\%$: (a) Soil 1; (b) Soil 2

experimental data points obtained using fibre-reinforced specimens are compared with the shear strength envelope predicted using the discrete approach proposed in this paper. The parameters for the equivalent shear strength of fibre-reinforced soil are also indicated in Table 3 (Series 12, 14, 16 and 18). The figure shows very good agreement between the experimental and predicted results, which provides added confidence in the use of the proposed discrete approach for a wide range of soils.

CONCLUSIONS

A discrete approach for fibre-reinforced soil was developed in this investigation. A major objective of the discrete framework is to avoid the need to conduct non-conventional shear strength testing programmes on fibre-reinforced specimens in order to perform limit equilibrium analyses. Instead, use of the discrete framework involves: (*a*) data provided to the geotechnical designer by the geosynthetic manufacturer regarding the properties of the fibre products; and (*b*) data

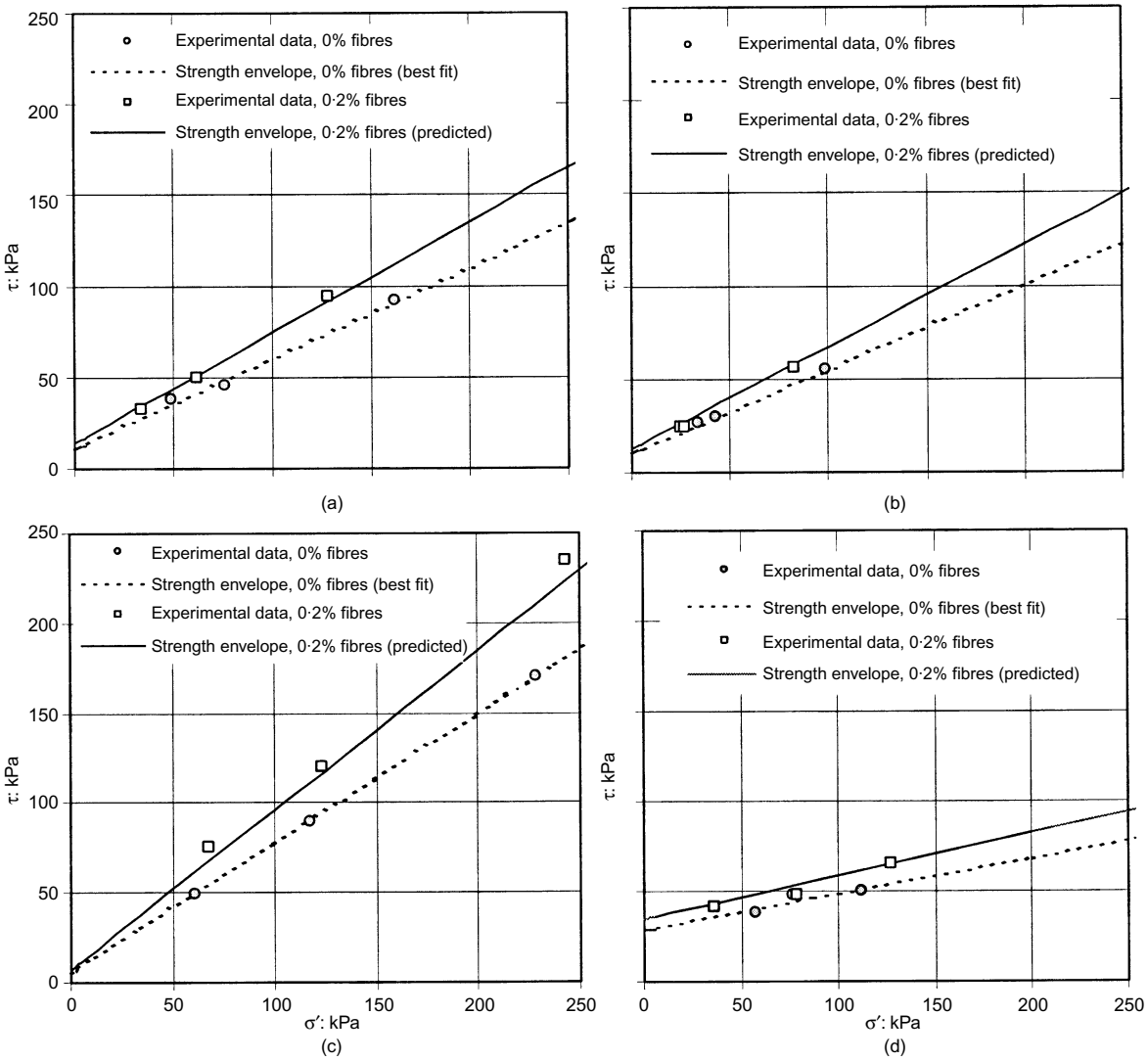

Fig. 11. Comparison between predicted and experimental shear strength results for specimens with 50 mm fibres placed at $\chi_w = 0{\cdot}2\%$: (a) Soil 3; (b) Soil 4; (c) Soil 5; (d) Soil 6

collected by the geotechnical designer on the shear strength of the candidate backfill soil. The discrete approach may also provide insight into the optimisation (e.g. optimised length, aspect ratio, surface characteristics) of fibre products used for soil slope stabilisation.

An experimental testing programme involving tensile testing of fibres and triaxial testing of unreinforced and fibre-reinforced specimens was undertaken to validate the proposed discrete framework. The testing programme involved different soil types, fibre contents, and fibre aspect ratios. The main conclusions drawn from this investigation are as follows:

(*a*) A discrete framework for fibre-reinforced soil could be developed such that the reinforced mass is characterised by the mechanical properties of individual fibres and of the soil, rather than by the mechanical properties of the fibre-reinforced composite material.

(*b*) A critical normal stress at which the governing mode of failure changes from fibre pullout to fibre breakage can be defined using the proposed discrete framework. The critical normal stress is a function of the tensile strength of the fibres, the soil shear strength, and the fibre aspect ratio, but is independent of the fibre content.

(*c*) According to the discrete framework, the fibre-induced distributed tension is a function of the fibre content, fibre aspect ratio, and interface shear strength of individual fibres if failure is governed by fibre pullout.

(*d*) According to the discrete framework, the fibre-induced distributed tension is a function of the fibre content and tensile strength of individual fibres if failure is governed by fibre tensile breakage.

(*e*) The discrete approach for fibre-reinforced soil predicts accurately the shear strength of specimens reinforced with polymeric fibres tested under confining stresses typical of slope stabilisation projects. As predicted by the discrete framework, the experimental results confirmed that the fibre-induced distributed tension increases linearly with fibre content and fibre aspect ratio when failure is characterised by pullout of individual fibres. Overall, good agreement of experimental results with analytic predictions was obtained for typical fibre geometries and fibre contents and for a wide variety of soil types.

ACKNOWLEDGEMENTS

Funding for this study was provided by Synthetic Industries, Inc. Additional support was provided by the National

Science Foundation under grant CMS-0086927. This assistance is gratefully acknowledged. The author is indebted to Dr Paula Pugliese and Mr Chunling Li for contributions in the analysis of experimental results, and to Dr Edward Kavazanjian Jr and Dr J. P. Giroud for their assistance during the compilation of early versions of this work. Finally, assistance provided by Mr Garry Gregory, Mr David Chill and Mr John Cannon on experimental components of this study is gratefully acknowledged.

NOTATION

a	adhesive component of interface shear resistance
A	control surface area
A_f	cross-sectional area of all fibres intersecting the control section
$A_{f,i}$	cross-sectional area of an individual fibre
c	soil cohesion
$c_{eq,p}$	cohesive component of equivalent shear strength when $\sigma_n < \sigma_{n,crit}$
$c_{eq,t}$	cohesive component of equivalent shear strength when $\sigma_n > \sigma_{n,crit}$
$c_{i,c}$	interaction coefficient of cohesive component of interface shear strength
$c_{i,\phi}$	interaction coefficient of frictional component of interface shear strength
d_f	equivalent diameter of a single fibre
f_f	interface shear resistance of individual fibres
G_f	specific gravity of fibres (dimensionless)
ld	linear density of fibres
l_e	embedment length of fibres
$l_{e,ave}$	average embedment length of fibres
l_f	total length of fibres
n	number of fibres intersecting control section
S	soil shear strength
S_{eq}	equivalent shear strength of fibre-reinforced soil
$S_{eq,p}$	equivalent shear strength when failure is governed by pullout of individual fibres
$S_{eq,t}$	equivalent shear strength when failure is governed by tensile breakage of individual fibres
t	fibre-induced distributed tension
$(\tan\phi)_{eq,p}$	frictional component of equivalent shear strength when $\sigma_n < \sigma_{n,crit}$
$(\tan\phi)_{eq,t}$	frictional component of equivalent shear strength when $\sigma_n > \sigma_{n,crit}$
t_p	fibre-induced distributed tension when failure is governed by pullout of individual fibres
t_t	fibre-induced distributed tension when failure is governed by tensile breakage of individual fibres
V	volume of fibre-reinforced soil
V_f	volume of fibres
W	weight of fibre-reinforced soil control volume
W_f	weight of fibres
W_s	dry weight of soil
α	empirical coefficient accounting for the direction of fibre-induced distributed tension ($\alpha = 1$ for randomly distributed fibres)
δ	friction angle characterising interface shear resistance
γ_d	dry unit weight of water of fibre-reinforced soil composite
γ_w	unit weight of water
η	aspect ratio of individual fibres
σ_1	major principal stress
σ_3	minor principal stress
$\sigma_{f,ult}$	ultimate tensile strength of an individual fibre
σ_n	normal stress acting on the shear plane
$\sigma_{n,ave}$	average normal stress acting on the fibres
$\sigma_{n,crit}$	critical normal stress
ϕ	soil friction angle
χ	volumetric fibre content
χ_w	gravimetric fibre content

REFERENCES

ASTM (1995). *Standard test method for unconsolidated undrained triaxial compression test for cohesive soils*, D4767-95. West Conshohocken, PA: ASTM International.

ASTM (1997). *Standard test method for tensile properties of yarns by the single-strand method*, D2256–97. West Conshohocken, PA: ASTM International.

ASTM (2000). *Standard test methods for laboratory compaction characteristics of soil using standard effort (12,400 ft-lbf/ft^3 (600 kN-m/m^3)*, D698-00a. West Conshohocken, PA: ASTM International.

ASTM (2001). *Standard test method for measuring geosynthetic pullout resistance in soil*, D6706-01. West Conshohocken, PA: ASTM International.

Consoli, N. C., Prietto, P. D. M. & Ulbrich, L. A. (1998). Influence of fibre and cement addition on behavior of sandy soil. *ASCE J. Geotech Geoenviron. Engng*, **124**, No. 12, 1211–1214.

Giroud, J. P. (1986). Geotextiles to geosynthetics: a revolution in geotechnical engineering. *Proc. 3rd Int. Conf. Geotextiles, Vienna*, 1–18.

Gray, D. H. & Al-Refeai, T. (1986). Behaviour of fabric versus fiber-reinforced sand. *ASCE J. Geotech. Engng* **112**, No. 8, 804–820.

Gray, D. H. & Ohashi, H. (1983). Mechanics of fiber-reinforcement in sand. *ASCE J. Geotech. Engng* **109**, No. 3, 335–353.

Gregory, G. H. & Chill, D. S. (1998). Stabilization of earth slopes with fiber-reinforcement. *Proc. 6th Int. Conf. Geosynthetics, Atlanta*, 1073–1078.

Koutsourais, M., Sandri, D. & Swan, R. (1998). Soil interaction characteristics of geotextiles and geogrids. *Proc. 6th Int. Conf. Geosynthetics, Atlanta*, 739–744.

Leflaive, E. (1985). Soils reinforced with continuous yarns: the Texol. *Proc. 11th Int. Conf. Soil Mech. Found. Engng, San Francisco* **3**, 1787–1790.

Maher, M. H. & Gray, D. H. (1990). Static response of sand reinforced with randomly distributed fibers. *ASCE J. Geotech. Engng* **116**, No. 11, 1661–1677.

Maher, M. H. & Ho, Y. C. (1994). Mechanical properties of kaolinite/fiber soil composite. *ASCE J. Geotech. Engng* **120**, No. 8, 1381–1393.

Maher, M. H. & Woods, R. D. (1990). Dynamic response of sand reinforced with randomly distributed fibers. *ASCE J. Geotech. Engng* **116**, No. 7, 1116–1131.

McGown, A., Andrawes, K. Z, Hytiris, N. & Mercel, F. B. (1985). Soil strengthening using randomly distributed mesh elements. *Proc. 11th Int. Conf. Soil Mech. Found. Engng, San Francisco* **3**, 1735–1738.

Michalowski, R. L. & Zhao, A. (1996). Failure of fiber-reinforced granular soils. *ASCE J. Geotech. Engng* **122**, No. 3, 226–234.

Mitchell, J. K. & Zornberg, J. G. (1995). Reinforced soil structures with poorly draining backfills. Part II: Case histories and applications. *Geosynthetics Int.* **2**, No. 1, 265–307.

Morel, J. C. & Gourc, J. P. (1997). Mechanical behavior of sand reinforced with mesh elements. *Geosynthetics Int.* **4**, No. 5, 481–508.

Ranjan, G., Vassan, R. M. & Charan, H. D. (1996). Probabilistic analysis of randomly distributed fiber-reinforced soil. *ASCE J. Geotech. Engng* **120**, No. 6, 419–426.

Shewbridge, S. E. & Sitar, N. (1990). Deformation based model for reinforced sand. *ASCE J. Geotech. Engng* **116**, No. 7, 1153–1170.

Wright, S. G. & Duncan, J. M. (1991). Limit equilibrium stability analyses for reinforced slopes. *Transp. Res. Rec.* **1330**, 40–46.

Zornberg, J. G. & Mitchell, J. K. (1994). Reinforced soil structures with poorly draining backfills. Part I: Reinforcement interactions and functions. *Geosynthetics Int.* **1**, No. 2, 103–148.

Zornberg, J. G., Sitar, N. & Mitchell, J. K. (1998). Limit equilibrium as a basis for design of geosynthetic reinforced slopes. *ASCE J. Geotech. Geoenviron. Engng* **124**, No. 8, 684–698.

Zornberg, J. G., Lafountain, L. & Caldwell, J. C. (2002). Analysis and design of an evapotranspirative cover for a hazardous waste landfill. *ASCE J. Geotech. Geoenviron. Engng*, in press.